Skull morphological variation in a British stranded population of false killer whale (*Pseudorca crassidens*, Owen 1846): a 3D geometric morphometric approach

Deborah Vicari[1], Richard C. Sabin[2], Richard. P. Brown[1], Olivier Lambert[3], Giovanni Bianucci[4] Carlo Meloro[1]

[1]Research Centre in Evolutionary Anthropology and Palaeoecology, School of Biological and Environmental Sciences, Liverpool John Moores University, Byrom Street, Liverpool L3 3AF, UK.

[2]Department of Life Sciences, The Natural History Museum, Cromwell Road, South Kensington, London SW7 5BD, UK.

[3]Institut Royal des Sciences Naturelles de Belgique, D.O. Terre et Histoire de la Vie, 1000 Brussels, Belgium.

[4]Dipartimento di Scienze della Terra, Università di Pisa, 56126 Pisa, Italy.

Correspondence

Deborah Vicari, Research Centre in Evolutionary Anthropology and Palaeoecology, School of Biological and Environmental Sciences, Liverpool John Moores University, Byrom Street, Liverpool L3 3AF, UK.

Email: D.Vicari@ljmu.ac.uk; D.Vicari@outlook.com

Running heading: False killer whale skull morphology

Abstract

The false killer whale *Pseudorca crassidens* (Owen, 1846) is a globally distributed delphinid, that shows geographical differentiation in its skull morphology. We explored cranial morphological variation in a sample of 85 skulls belonging to a mixed sex population stranded in the Moray Firth, Scotland in 1927. Microscribe 3D 2GX was used to record 37 anatomical landmarks on the cranium and 25 on the mandible in order to investigate size and shape variation and to explore sexual dimorphism using geometric morphometric. Males showed greater overall skull size than females whilst no sexual dimorphism could be identified in cranial and mandibular shape. Allometric skull changes occurred in parallel for both males and females supporting the lack of sexual shape dimorphism for this particular sample. Also, fluctuating asymmetry did not differ between crania of males and females. This study confirms the absence of sexual shape dimorphism and the presence of a sexual size dimorphism in this false killer whale population.

Keywords: toothed whale, morphology, asymmetry, partial least squares, false killer whale.

Introduction

The false killer whale, *Pseudorca crassidens* (Owen, 1846) is a large cetacean with a cosmopolitan distribution that ranges mainly between 50°N and 50°S in latitude (Baird 2009a). Adults can reach total body lengths (TBL) of 5m (females) to 6m (males), making this species one of the largest members of the Delphinidae family (Baird 2009a). Together with the true killer whale (*Orcinus orca*), *P. crassidens* shows an occasional tendency to eat marine mammals such as small and large cetaceans (Alonso et al. 1999; Odell and McClune 1999; Baird 2009a) although their main prey is squid and fish (Alonso et al. 1999; Baird 2009a).

Morphological variation in the false killer whale is poorly understood and there have been few studies on the skull morphology of this large odontocete. The skull has conical and large teeth, and the tooth count is 7-11 for each of the upper jaws and 8-12 for the lower jaws (Yamada 1956; Baird 2009a). A previous analysis from a stranded false killer whale population described a degree of sexual dimorphism in body size with males generally larger in overall body length and weight (Baird 2009a). Mead (1975) and Baird (2009a) also reported differences in the shape of the head due to the melon that is generally more pronounced in males than in females. Since the melon is an organ of sound production and transmission it is likely that this is associated with sexual differences in false killer whale echolocation.

Skull shape can be a good proxy for understanding factors which influence variation (sexual or ecogeographical) in the false killer whale as demonstrated for other cetacean species (see: del Castillo et al. 2014, 2016, 2017). To date, only one study has identified skull sexual dimorphism and population differences in *P. crassidens* based on specimens from South Africa and Scotland (Kitchener et al. 1990). The authors detected significant sexual differences in the length of the rostrum, the ventral cranium and the temporal fossa. Another study on growth pattern in Japanese and South African false killer whales identified that at sexual maturity, South African whales were smaller than Japanese whales, and males from both populations were larger than females (Ferreira et al. 2014). Scottish individuals measured by Kitchener et al. (1990) were generally larger than the South African individuals and closer in body size to the Japanese population (Ferreira, 2009). No other published study has described skull size and shape variation in this species.

Geometric morphometrics (Rohlf and Marcus 1993) can be a useful tool for studying skull morphological variation (Marcus et al. 2000). This method quantifies size and shape variation via the digitisation of spatial coordinates belonging to a set of anatomically and/or

geometrically defined homologous landmarks (2D/3D) on biological specimens (Adams et al. 2004; Adams and Otárola-Castillo 2013). Previous geometric morphometric approaches on cetaceans have successfully separated geographic populations, ontogenetic groups, sexes and species in many odontocetes (Monteiro-Filho et al. 2002; Westgate 2007; Nicolosi and Loy 2010; Loy et al. 2011; Wiig et al. 2012; del Castillo et al. 2014) and so it stands to reason that these methods can successfully identify size and/or shape affinities/disparities between male and female false killer whales.

Using geometric morphometrics, this study aims to address the following research questions pertinent to *P. crassidens*:

1. To what extent does a single population display intraspecific morphological variation in the skull? Are skull size and skull shape sexually dimorphic? It is expected that skull sizes of false killer whales will exhibit a significant degree of sexual dimorphism (Kitchener et al. 1990; Ferreira et al., 2014), whilst dimorphism in skull shape might be subtle and difficult to identify (Loy et al. 2011).

2. Do males and females show differences in the degree of cranial asymmetry? Previous morphological studies on toothed whales showed differences in the degree of directional asymmetry (Fahlke and Hampe 2015; Coombs et al., 2020), related to prey size (MacLeod et al. 2007; McCurry et al. 2017) and suction feeding abilities (del Castillo et al. 2017). Differences between sexes have been found in the nasal area of the pontoporiid *Pontoporia blainvillei* (del Castillo et al., 2014), which might be related to their vocalization abilities. Based on this, we might expect a difference in the degree of cranial asymmetry between males and females of *Pseudorca crassidens*.

3. Do males and females show differences in the degree of skull integration (Klingenberg 2009)? It is predicted that integration/modularity between crania and mandibles should occur in both sexes. Previous morphological studies on mammals (Zelditch and Carmichael 1989; Marroig and Cheverud 2001; Hallgrímsson et al. 2002; Klingenberg et al. 2003; Klingenberg 2008; Willmore et al. 2009; Figueirido et al. 2013; Veneziano et al. 2018) showed a significant degree of association between cranial and mandibular morphology at both intra and interspecific scales. However, not many studies have yet explored patterns of integration in cetaceans (Churchill et al. 2019). Since they do not chew their food extensively and their mandibles are also involved in sound reception (Cranford et al. 2008, 2015; Cranford and Krysl 2018), different levels of integration are expected, compared with other mammal groups. Additionally, if diet and sound reception differ between sexes it might be possible that the level

of integration also shows some degree of differentiation between sexes. Alternatively, these similarities might indicate a similar specialization through feeding adaptations.

Materials and Methods

Samples- We examined 85 crania (♂=37; ♀=39; No Data available – ND = 9; (**Appendix 1**); and 29 complete skulls (combined cranium and mandibles; ♂=12; ♀=17) of *Pseudorca crassidens* housed at the Natural History Museum, London, UK (**Appendix 1**)**.** Though these specimens have two different groups of catalogue numbers – 1961 and 1992, all are considered related to a mass-stranding event which took place in October 1927 at the Dornoch Firth, Scotland. Specimens labelled 1992 were collected from Ardgay Bay and along the Kyle (a narrow sea channel) beyond Bonar Bridge to Invershin. Donorch Firth is part of the larger Moray Firth embayment located on the east coast of the Highlands in the north of Scotland. Information regarding the gender of all six specimens with the catalogue number 1992 and the two within the sample with catalogue number 1961 are missing (see **Appendix 1**). The majority of the samples were considered as adults, but we identified two as subadults because the maxillary bones did not reach the nuchal crest caudally and the frontal bones were visible in dorsal view (Cozzi et al. 2016).

Sampling- Three dimensional (3D) coordinates of 37 anatomically-defined homologous landmarks were placed on 85 crania (**Figure 1**; **Table 1**), and twenty-five landmarks were placed on 29 mandibles (**Figure 1**; **Table 2**) using Microscribe G2X at an accuracy of 0.23 mm (Immersion Corp., San Jose CA, USA). Due to the large size of the specimens two landmarking sessions for each specimen were recorded by the same researcher (DV) on the cranium in order to cover both dorsal and ventral parts. These were then merged using DVLR software (Dorsal-Ventral-Left-Right fitting, http://www.nycep.org/nmg). Coordinates on mandibles were captured in a single landmarking session by the same researcher (DV). Landmarks were imported into Morpheus 20140704 (Slice 2014) and MorphoJ 1.06d (Klingenberg 2011) to ensure that all the 3D spatial coordinates were captured in an identical, sequential order.

Measurement error- To explore the degree of measurement error introduced by the 3D landmarking, linear measurements between selected anatomical landmarks were taken with a measuring tape on crania (accuracy of 0.1 mm), and successively compared with inter-landmark distances taken on the dorsal and ventral views and on the combined landmarks

configurations with DVLR. To test the Microscribe degree of accuracy during the data collection, the spatial position of 18 equally distant (=1 cm) points along a scale bar 5cm by 3cm were taken right before the beginning of each landmarking session on crania. The distances between the selected 18 points were checked to ensure accuracy of the spatial coordinates. In all cases the distances obtained using the microscribe showed an error of <5% compared to the values of the scale bar. To evaluate the reliability of the landmark configuration, a repeatability index (*R*) was calculated on 85 crania using the Procrustes ANOVA (analyses of shape variance) in MorphoJ 1.06d. The operator (DV) digitized each cranium twice and followed standard protocol procedures and analyses described in Fruciano (2016), and Cardini (2014) in order to ensure that the shape variance explained by the replica was significantly smaller than that exhibited by individuals. This was accomplished using a Procrustes ANOVA in MorphoJ 1.06d (Klingenberg 2011), a method adapted for the study of shape variation (Klingenberg and McIntyre 1998; Klingenberg et al. 2002) equivalent to a two-way ANOVA (Palmer and Strobeck 1986) with individuals and replicas as factors, and shape coordinates (see next section) as dependent variable. The repeatability index *R*, which varies between 0 (not repeatable) and 1 (perfectly repeatable), was equally computed based on the comparison of shape variation between the first and the second landmarking session following Fruciano (2016).

Geometric Morphometrics (GM)- Landmarks of crania and mandible were separately superimposed using a Generalised Procrustes Analysis (GPA) which removes the effects of differences in size, position, and orientation from the 3D spatial coordinates (Rohlf and Marcus 1993). This is an iterative procedure where variation in size is first removed by scaling each configuration so that it has a centroid size (CS = the square root of the sum of squared distances between each landmark and the centroid) equal to 1.0; rotation and translation are taken into account by centring and rotating the landmark configuration in order to obtain an optimal solution that minimizes the quadratic distances between homologous points (Bookstein 1997). After GPA, a new set of coordinates (named Procrustes) are created and then used as a proxy for shape variables to explore the potential for differences in cranial and mandibular morphology between sexes, separately.

Data analyses on 3D crania and mandibles- GM permits partitioning of the asymmetric and symmetric components of shape variation (Klingenberg et al. 2002). As many species of odontocetes show a high degree of directional asymmetry in their crania (MacLeod 2002; Fahlke et al. 2011; Fahlke and Hampe 2015; Huggenberger et al. 2017; Churchill et al. 2019),

and the asymmetric component is relevant for the aim of the study, these variables were partitioned following the guidelines of Klingenberg et al. (2002).

Procrustes ANOVA (analysis of shape variance) was performed on 85 crania replicates to investigate the presence of Directional (DA) and Fluctuating Asymmetry (FA) in cranium shape using MorphoJ 1.06d (Klingenberg 2011). DA is defined as a deviation from symmetry showed in most of the individuals belonging to the same species (MacLeod et al. 2007). FA can be defined as the difference in mean absolute value of left and right sides in the same individual (Klingenberg et al. 2002). When the mean value is close to zero, it means that the structure shows an almost perfect symmetry (Tomkins and Kotiaho 2001). FA scores were quantified in each individual in units of Procrustes and Mahalanobis distances. While FA Procrustes distances are calculated as individual deviation from the mean asymmetry to the absolute shape, Mahalanobis distances are quantified as individual deviation from the mean asymmetry in the sample (Klingenberg and Monteiro 2005). A two-independent-sample *t*-test was performed to assess possible sexual differences in FA scores of the crania. Because odontocete mandibles are generally considered symmetrical (Barroso et al. 2012), the full shape of the mandible was captured without separating symmetric from the asymmetric component.

To explore the degree of intraspecific asymmetric and symmetric shape variation in the 85 crania and full shape variation in the 29 mandibles, Principal Component Analysis (PCA) was performed separately for crania and mandibles using the functions bilat.symmetry and plotTangentSpace, respectively in the geomorph 3.1.2 package (Adams et al. 2016) within R 3.5.2 (R Core Team 2018). To aid identification of different skull shapes within sexes, a permutation test (1,000 permutations) on Procrustes distances and a Discriminant Function Analysis (DFA) were also performed in MorphoJ 1.06d (Klingenberg 2011) for the mandibles and crania datasets separately. This analysis uses the differences between means of Procrustes and Mahalanobis distances to classify the specimens in two groups (males and females); a significant *p*-value will be associated with a significant degree of sexual dimorphism in shape.

ANOVA and Procrustes ANOVA (using the function procD.lm of geomorph 3.1.2) were additionally performed on the 74 sexed crania and 29 sexed mandibles to test for sexual dimorphism in skull size (SSD) and shape, respectively. The same function was employed to test allometry (the impact of size on shape variation) with log transformed CS as *X* and symmetric shape component as *Y*. Slope differences between sexes were explored adding sex

as a factor in the model 'shape~size' and testing the interaction term 'size*sex'. Analyses on the sexed crania were run after the exclusion of two subadult (male) specimens. This was done to give the same range of size for both sexes as this dataset did not include female subadults. In the case of common allometric patterns being found between the sexes, residuals (or size free variables) were used for further analyses of sexual dimorphism. Additionally, a between-sex ANOVA was also performed on Total Body Length (TBL) – information collected after stranding and stored in the NHM database – as comparison with CS values from the skull. CS and TBL were summarized using boxplots and the significance of differences between sexes was tested using *t*-tests against the null hypothesis of being no difference between means for either variable.

Patterns of covariation between cranium and mandibular shape were examined using two-blocks Partial Least Squares (2B-PLS) analysis (Zelditch et al. 2012, 2013) pooled within sexes in a dataset of 29 complete skulls (the combined cranium and mandible). PLS is a useful method for studies investigating integration/modularity between two different blocks of variables (Klingenberg 2009; Zelditch et al. 2012; Klingenberg and Marugán-Lobón 2013), such as the mandible and cranium shape in this instance. Unlike the PCA, the PLS method uses singular value decomposition (SDV) to identify vectors called singular axes (SAs; Zelditch et al. 2012), which explains covariance in the same way that PCA explains variance. Unlike the PCs, SAs are paired, and each SA score accounts for the covariance between blocks (Klingenberg 2009; Zelditch et al. 2012). Differences in covariation trajectories between sexes were tested using angular comparison of the PLS vectors in MorphoJ 1.06d (Klingenberg 2011; Klingenberg and Marugán-Lobón 2013) against the null hypothesis of no difference from two random orthogonal vectors (90 degrees). Therefore, a significant *p*-value will reflect a statistically more similar shape variation than two random vectors. In contrast, a non-significant *p*-value will indicate different directionalities in shape between sexes. PLS analyses were applied to male and female datasets separately, and the angle between each PLS of each dataset was calculated. Like the PCs, SAs can be described by deformation along axes, which helps with the interpretation of the results (Zelditch et al. 2012). The null hypothesis of no covariation between cranium and mandible was tested with 1,000 resamples. (Zelditch et al. 2012, 2013). Unlike the angular comparison between PCs in between sexes, differences in directionalities of PLS vectors are not indicative of different shapes but of different patterns of integration between sexes.

Results

Cranial dataset

Measurement error- The Procrustes ANOVA (**Table 3**) showed significant effects of individuals on shape as well as side, representing Directional Asymmetry (DA), and the interaction between individual and side, representing Fluctuating Asymmetry (FA). Sum of squares (SS) was greater in DA and smaller in the landmarking error, suggesting a negligible impact of landmarking on shape variation. This was equally confirmed by the Repeatability (*R*) score for shape that was 0.95.

Asymmetric component- In the PCA of the asymmetric component of shape, PC1 summarized 29.4% of the variation (**Figure 2A**). Along this axis, individuals that are located towards the negative region show an accentuation of DA, while those in the positive region of the axis have less asymmetrical crania. Males and females showed no differences in the average of FA scores no matter whether Mahalanobis (p=0.2451) or Procrustes FA scores (p=0.9847) were considered (**Figure 3**).

Symmetric component- PC1 and PC2 (**Figure 2B**) on the symmetric component of shape accounted for 19% and 12% of variance, respectively (**Appendix 2**). PC1 positive scores correspond to a more laterally compressed facial region, an area bounded posteriorly by the dorsal apex of the nuchal crest defined by landmark 10. PC1 negative scores represent a shorter rostrum and a transverse widening of the neurocranium, resulting in a more tapered skull shape. For the area of the occipital condyles described by seven landmarks (LM 15, 16, 17, 18, 19, 20, 21), negative PC scores represent a wider shape together with an enlargement of the medial wall of the temporal fossa formed by a small portion of the squamosal (squamosal plate) and by the parietal described by three landmarks (LM 12, 14, 27). The PC2 axis describes changes in the curvature of the rostrum profile and the position of the neurocranium relative to the rostrum. PC2 negative scores reflect a high degree of curvature in the skull profile and a wider neurocranium with the displacement of landmarks 10, 11, and 12. Landmarks 10 and 7 are further apart compared to PC2 positive scores. The plot of PC1 against PC2 (**Figure 2A**) indicated considerable male-female overlap in the morphospace. When distances between groups were compared by a linear DFA, there was no significant distance between sexes (p= 0.23). Equally, Procrustes ANOVA highlighted no significant (p= 0.132) difference in cranium shape between males and females (**Table 4**).

Allometry-The regression of Procrustes coordinates versus CS revealed a significant (p=0.001) allometric component in cranium shape, with size explaining 44% of variance (**Table 5**) of the pooled sample. Procrustes ANOVA revealed no difference between sex allometric slopes for CS ($F_{2,74}$=1.1692, p=0.259; **Table 5**) or TBL ($F_{2,74}$=0.8252, p= 0.661*;* **Table 5**). When allometric trajectories were individually analysed for males and females it was possible to note a significant impact of size on shape that explained 16.34% of variance in males (n = 37; p < 0.001), and 12.59% of variance in females (n= 39, p < 0.001). The angle vector was 26.13° with p < 0.001, meaning that the two vectors are pointing in the same direction, and they have similar allometric trajectories. A test for differences between sexes using cranial and residuals shape variables of allometry confirmed no difference in shape between males and females (p= 0.057, **Table 4**). On the other hand, a boxplot showed greater values for cranium CS and TBL in male specimens confirmed by *t*-tests (CS: p=0.007; TBL: p= 0.05) (**Figure 4A-B**).

3D Mandibles dataset

Shape analyses- PC1 and PC2 accounted for 42.8% of the total variance (**Figure 5; Appendix 3**) and showed mixed scores belonging to male and female specimens. Positive scores on PC1 describe a lengthened mandible, represented by a forward shift of landmarks 6 and 7 that represent the most anterior point of the mandibular foramen on the medial side or the acoustic window on the lateral side (Mead and Fordyce 2009). The right and left sides of the mandibular foramen show a different angle compared to PC1 negative values. The hemi-mandibles create a more obtuse angle on PC1 positive values, and the mandible appears more elongated (**Figure 5,** wireframe in occipital, ventral and lateral view). Also, positive values on PC1 represent a backward shift in the space of the landmarks 4 and 5 describing the posterior end of the dental groove on the alveolar border of the mandible, while landmarks 12 and 13 (the coronoid process) shift upward. PC2 describes the curvature of the mandible, with negative values showing a more convex dorsal margin and larger mandibular body. A permutation test based on Procrustes distances highlighted no differences in mandible shape between males and females (p = 0.9864). This was equally confirmed by DFA (p = 0.8962). Procrustes ANOVA on the total sample of 29 specimens showed that size explained 5.8% of total mandible shape variance (**Table 6**), although this was not significant and a significant effect was neither detected for sex (**Table 6**). If TBL was considered as a factor against mandibular shape, rather than CS, the result was unaffected (**Table 6**). Both CS and TBL demonstrated that males were generally larger than females (**Figure 4C-D;** CS: p=0.007; TBL: p=0.01).

Cranial and Mandibular Integration

The 2B-PLS analysis is shown in **Figure 6**. The first pair of SAs account for 62.52% of the total squared covariance between cranium and mandible. Although high (r = 0.795), the strength of association between scores of cranium and mandible shape was not significant (p= 0.081*)*.

2B-PLS for females (n=18?) showed a significant (p= 0.0014) correlation (RV= 0.5093) between cranium and mandible shape, while in males (n = 11) the correlation between these two anatomical units was non-significant (p= 0.0799) even if the correlation coefficient was higher (RV= 0.6336). Comparing the cranium axis of males and females, PLS1 showed an angle of 56.937°, and PLS2 an angle of 57.603°, and both were significant ($p < 0.00002$; p = 0.00003; **Table 7**). Similar results were obtained for the mandible, with PLS1 showing an angle of 38.785°, and PLS2 an angle of 60.013° ($p< 0.00001$; p= 0.00223*;* **Table 7**).

Discussion

The investigation of sexual dimorphism in the morphology of cetaceans might give insights into their social structure, breeding behaviours and foraging. In this study, we identified a significant level of sexual dimorphism in the general size of the body, cranium, and mandible of the large delphinid *Pseudorca crassidens*. On the other hand, the shape traits separately investigated for the cranium and the mandible showed no difference between males and females, and the two groups appear to have similar allometric trajectories.

These results are consistent with Kitchener et al. (1990), who found that males of *P. crassidens* were characterised by larger crania and mandibles compared to females. Equally, fieldwork data support our findings on total body length, but not on cranial shape considering that significant sexual differences in the external head shape (including soft tissues) of *P. crassidens* have been described (Stacey et al. 1994). The absence of skull shape sexual dimorphism seems to be common in cetacean species that live in large monospecific groups (de Francesco and Loy 2016). This might be partly related to the conservative social structure that both males and females maintain for niche partitioning during aquatic foraging or could instead be related to food sharing within the group (Baird 2009a; Ralls and Mesnick 2009). Adult specimens generally show an enlargement of the area of the temporal fossa (formed by the alisphenoid, frontal, parietal and squamosal bones). Having a large temporal area allows for a larger attachment surface of the temporalis muscle (Cozzi et al. 2016), associated to the production of stronger bite forces. A reduction in the size of this area would cause the mouth to close faster

(i.e. in subadults specimens) at the expense of the bite force, because force and velocity are inversely proportional with a well-established trade-off (Marshall 2009). The temporal muscle is inserted along the dorsal ridge of the mandible, with a stronger and somewhat tendinous attachment over the coronoid process (landmarks 12 and 13) and a weaker attachment anteriorly along the dorsal margin of the mandibular foramen (Seagers 1982). The area of the temporal fossa can be used to predict prey size, bite strength, and grip and tear feeding mode (Marshall 2009; Galatius et al. 2020). If this area had been greater in males, it may have testified for a male-male aggression character related to sexual dimorphism (Cozzi et al. 2016).

To date little is known about male and female *P. crassidens* social behaviour. In general, males and females share the same diet and exhibit high fidelity to the natal group (Martien et al. 2011). They feed on a variety of squid, fish, and occasionally mammals such as the sperm whale and delphinids (Stacey et al. 1994; Palacios and Mate 1996; Odell and McClune 1999; Baird 2009a). They catch their food mostly during the day, exceeding then dive depths of 200m, and tend to remain at shallow depths during the night (Baird 2009b; Minamikawa et al. 2013). Prey specialisation has also been suggested in different populations (Ferreira 2008; Botta et al. 2012).

The absence of sexual shape dimorphism or monomorphism in *P. crassidens* might be due to their ability to socialize and share food resources within the pod (Stacey et al. 1994; Odell and McClune 1999; Baird 2009a). This has been confirmed by stable isotope studies (Botta et al. 2012; Riccialdelli and Goodall 2015). Similar to the results presented here, previous studies on other, smaller delphinids such as *Cephalorhynchus commersoni*, *Tursiops truncatus*, *Delphinus delphis*, *Stenella coeruleoalba* and *S. attenuata* (Clark and Odell 1999; Wilson et al. 1999; Sanvicente-Añorve et al. 2004; Murphy and Rogan 2006; Amaral et al. 2009; Parés-Casanova and Fabre 2013; del Castillo et al. 2016) found no sexual dimorphism in skull shape, suggesting that males and females might have similar feeding behaviours (MacLeod et al. 2006).

Asymmetry - In this study the percentage of variance explained by DA was greater than FA. As the odontocete ccranium shows asymmetry related to the production of echolocation high frequency sounds (Cranford et al. 1996; Fahlke and Hampe 2015; Cozzi et al. 2016; Coombs et al. 2020), these results agree with expectations based on previous studies (del Castillo et al. 2014, 2016, 2017). The DA accounted for 25% and the FA for 10% of total shape variation in *P. crassidens* (**Table 3**). Similar results for FA were found for *Lagenorhynchus australis* (8.5%; del Castillo et al. 2017), *Lagenorhynchus obscurus* (9.5%; del Castillo et al. 2017), and

Cephalorhynchus commersoni (10%; del Castillo et al. 2016). Also, in these species the DA accounted for 43%, 25%, and 34% respectively (del Castillo et al. 2017); *P. crassidens* shows a variation similar to *L. obscurus* but lower variation compared to *L. australis* and *C. commersoni*. Therefore, the DA can be argued to be functionally linked to both echolocation (Fahlke and Hampe 2015) and prey size (MacLeod et al. 2007; McCurry et al. 2017). In fact, the two sympatric species *L. osburus* and *L. australis* showed a different degree of DA and different suction feeding abilities (del Castillo et al. 2017). In Lissodelphininae there is variation in the magnitude of directional asymmetry between species, and this variation is related to ecological partitioning (Galatius and Goodall 2016; del Castillo et al. 2017). The nasal area is the most affected area by the asymmetric component (**Figure 2B**) in both males and females of *P. crassidens*. This is in line with the pontoporiid *Pontoporia blainvillei* which showed DA differences in the bony nares region between sexes, probably due to a different vocalization (del Castillo et al. 2014). Different fluctuating asymmetry scores have not been detected in false killer whale females and males (**Figure 5**). For this reason, differences in the shape of the head between sexes are most likely related to the shape of soft tissues, such as the melon, involved in emission beam production, although this cannot be tested with our dataset.

Sexual size dimorphism (SSD)- Sexual size dimorphism can be described as the difference between features such as body size between males and females (Ralls and Mesnick 2009). SSD can evolve for different reasons and can be explained by factors such as age at sexual maturity, mating system, contest competition, female choice, and sound production.

Size explained a significant part of the total variation in cranial shape (4 %); this is a lower percentage if compared with other toothed whales (i.e *Cephalorhynchus commersoni*; 5.7%; del Castillo et al. 2016; *P. blainvillei*; 54.1% del Castillo et al., 2014). Considering that our sample did not include ontogenetic groups, the obtained result is not surprising and in line with other studies that explored allometric variation only in adults (De Francesco and Loy, 2016). Female false killer whales in Scotland attain sexual maturity earlier than males (Purves and Pilleri 1978). Whilst males reach maturity when their body length is 396-457 cm, roughly around the age of 11-18 (Kitchener et al. 1990; Stacey et al. 1994), females reach maturity between the ages of 8-11 (Ferreira et al. 2014) and 336 cm of body length (Stacey et al. 1994). Their breeding age range is similar to *Orcinus orca* (Ottensmeyer and Whitehead 2003): males stop growing after 15 years of age (Duffield 1988) and females reach reproductive age earlier than males. Males might not provide parental care for calves and, instead, invest that energy in growth (Nowak and Walker 1999). In addition, having males with a larger body size can

increase their ability to dive to greater depths (Beck et al. 2003; Baird et al. 2005; Piscitelli et al. 2010; Riccialdelli and Goodall 2015; Goldbogen et al. 2019). In cetaceans, this delay in male maturation is also related to a polygynous mating system (some males with multiple partners), while the absence of sexual dimorphism is related to a polygynandrous mating system (males and females have multiple partners) (Mesnick and Ralls 2018; Murphy et al. 2005). Both strategies are associated with male sperm competition (Mesnick and Rall 2018), and are interpreted as a way to increase fitness and genetic variability through the offspring (Stockley, 2004).

Food intake in two females and one male of false killer whales in captivity indicates an increase in annual food consumption for the male from the fourth to the sixth years of age (Kastelein et al. 2000). This might confirm the hypothesis that males use the energy to grow and increase their body size, whilst females use the energy to take care of the offspring. Sexual size dimorphism with males larger than females has also been observed in *Lagenorhynchus* spp. (Reeves et al. 1999; Galatius 2010; del Castillo et al. 2017), *Lissodelphis borealis* (Mesnick and Ralls 2018), *Tursiops truncatus* (Tolley et al. 1995; Amaral et al. 2009; Parés-Casanova and Fabre 2013), *Orcinus orca*, *Globecephala* spp. (Mesnick and Ralls 2018), among the other delphinids, in the monodontids *Delphinapterus leucas* (Mesnick and Ralls 2018) and *Monodon monoceros* (Garde et al. 2007; Mesnick and Ralls 2018), in the ziphiid *Mesoplodon densirostris,* in the physeterid *Physeter macrocephalus* (Mesnick and Ralls 2018), and in the iniid *Inia geoffrensis* (Mesnick and Ralls 2018). Instead, a reversed sexual dimorphism, with females being larger than males, has been observed in *Cephalorhynchus* spp. (del Castillo et al. 2016; Mesnick and Ralls 2018) among the other delphinids, in the phocoenids *Phocoena phocoena* and *P. sinus* (Mesnick and Ralls 2018), in the pontoporiid *Pontoporia blainvillei* (Ramos et al. 2002; del Castillo et al. 2014; Mesnick and Ralls 2018), in the ziphiid *Berardius spp.* (Mesnick and Ralls 2018), in the recently extinct *Lipotes vexillifer* (Mesnick and Ralls 2018), and also in 13 mysticete species (Ralls and Mesnick 2009). In *P. phocoena*, females are larger than males, which provides to the former a higher reproducibility potential for annual reproduction (Read and Gaskin 1990; Galatius 2010; Gol'din and Vishnyakova 2016). Females of *P. phocoena* reach sexual maturity later than males (Sørensen and Kinze 1994; Mclellan et al. 2002; Lockyer 2003; Lockyer et al. 2003; Marino et al. 2004), can better compete for resources, and their calves have a more adequate size to maintain body temperature (Ralls 1976).

Body size changes can also be related to biosonar types (Jensen et al. 2018) and communication sounds, with sexual dimorphism being observed for calls , such as in *Globicephala melas* (Ralls and Mesnick 2018), or on emission beam patterns (Au et al. 1995; Kloepper et al. 2012). Most of the largest odontocete species were recognized as having the greatest degree of SSD: *Physeter macrocephalus*, *Orcinus orca*, *Hyperoodon* spp., *Monodon monoceros*, *Delphinapterus leucas*, *Globicephala* spp., *Berardius bairdii*, *Ziphius cavirostris*, and *Mesoplodon* spp. (Cranford 1999; MacLeod and MacLeod 2009; Ralls and Mesnick 2009; MacLeod 2010; Goldbogen et al. 2019). A known trend is that the larger the animal, the louder sound it will produce (Ralls and Mesnick 2009). False killer whales are extremely vocal (Murray et al. 1998) and differences in vocalization were recorded between populations but not between sexes (Rendell et al. 1999; Oswald et al. 2003; Sanino and Fowle 2006; Barkley et al. 2019).

The allometric parallel slopes observed for males and females showed that the directions of shape changes in the cranium are conserved among sexes. As morphological changes can also be associated with phylogenetic differences (Galatius et al., 2020) in size within Delphinidae (evolutionary allometry), allometric trajectories should be analysed in the whole context of toothed whale evolution to understand if those trajectories tend to differ along with the increasing of the divergence time between different species of delphinids/odontocetes. Describing these patterns will deepen our knowledge of the underlying macroevolutionary processes in Delphinidae and Odontoceti.

Conclusion

In conclusion, although false killer whales are sexually dimorphic in the external shape of the head (Stacey et al. 1994), this study showed sexual size dimorphism but no sexual skull shape dimorphism. Combining the results and the interpretations above, it is likely that false killer whales are polygynandrous (Nowak and Walker 1999; Shirihai 2006), with males being larger than females, but both sexes sharing food resources (Botta et al. 2012; Riccialdelli and Goodall 2015). Using isometric-free 3D variables, this study provides new insights into cranial asymmetry in individuals belonging to the same population. In addition, exploring FA proxies and the related skull traits between populations might prove an important area for future research. Moreover, further studies using stable isotopes and DNA analyses from these specimens might further improve our understanding of the ecology and genetics of false killer whale populations.

Acknowledgements

The authors are grateful to the staff of Natural History Museum (NHM) for assistance and access to cetacean collection. Andrea Cardini and Davide Tamagnini equally supported us during data analyses and interpretation. This work was supported by Liverpool John Moores University (LJMU) PhD scholarship research grant. We thank the two anonymous reviewers for their valuable comments.

Author contributions

D.V. collected the data and performed the statistical analyses. D.V. together with C.M., R.S., O.L., G.B., R.P.B. wrote and revised the manuscript. R.C.S. helped D.V. during data collection at NHM. C.M. supervised the project.

Competing interests: The authors declare there are no competing interests.

References

Adams, D.C., Collyer, M., Kaliontzopoulou, A., and Sherratt, E. 2016. Geomorph: Software for geometric morphometric analyses. Comprehensive R Archive Network.

Adams, D.C., and Otárola-Castillo, E. 2013. geomorph: an R package for the collection and analysis of geometric morphometric shape data. Methods Ecol. Evol. **4**(4): 393–399. Wiley Online Library.

Adams, D.C., Rohlf, F.J., and Slice, D.E. 2004. Geometric morphometrics: ten years of progress following the 'revolution'. Ital. J. Zool. **71**(1): 5–16. Taylor and Francis.

Alonso, M.K., Pedraza, S.N., Schiavini, A.C.M., Goodall, R.N.P., and Crespo, E.A. 1999. Stomach contents of false killer whales (Pseudorca crassidens) stranded on the coasts of the Strait of Magellan, Tierra del Fuego. Mar. Mammal Sci. **15**(3): 712–724. Wiley Online Library.

Amaral, A.R., Coelho, M.M., Marugán-Lobón, J., and Rohlf, F.J. 2009. Cranial shape differentiation in three closely related delphinid cetacean species: Insights into evolutionary history. Zoology **112**(1): 38–47. Elsevier.

Au, W.W.L., Pawloski, J.L., Nachtigall, P.E., Blonz, M., and Gisner, R.C. 1995. Echolocation

signals and transmission beam pattern of a false killer whale (Pseudorca crassidens). J. Acoust. Soc. Am. **98**(1): 51–59. ASA.

Baird, R.W. 2009a. False killer whale: Pseudorca crassidens. *In* Encyclopedia of marine mammals. Elsevier. pp. 405–406.

Baird, R.W. 2009b. A review of false killer whales in Hawaiian waters: biology, status, and risk factors. Cascadia Research Collective Olympia.

Baird, R.W., Hanson, M.B., and Dill, L.M. 2005. Factors influencing the diving behaviour of fish-eating killer whales: sex differences and diel and interannual variation in diving rates. Can. J. Zool. **83**(2): 257–267. NRC Research Press.

Barkley, Y.M., Oleson, E.M., Oswald, J.N., and Franklin, E.C. 2019. Whistle classification of sympatric false killer whale populations in Hawaiian waters yields low accuracy rates. Front. Mar. Sci. **6**: 645. Frontiers.

Barroso, C., Cranford, T.W., and Berta, A. 2012. Shape analysis of odontocete mandibles: functional and evolutionary implications. J. Morphol. **273**(9): 1021–1030. Wiley Online Library.

Beck, C.A., Bowen, W.D., McMillan, J.I., and Iverson, S.J. 2003. Sex differences in the diving behaviour of a size-dimorphic capital breeder: the grey seal. Anim. Behav. **66**(4): 777–789. Elsevier.

Bookstein, F.L. 1997. Morphometric tools for landmark data: geometry and biology. Cambridge University Press.

Botta, S., Hohn, A.A., Macko, S.A., and Secchi, E.R. 2012. Isotopic variation in delphinids from the subtropical western South Atlantic. Mar. Biol. Assoc. United Kingdom. J. Mar. Biol. Assoc. United Kingdom **92**(8): 1689. Cambridge University Press.

Cardini, A. 2014. Missing the third dimension in geometric morphometrics: how to assess if 2D images really are a good proxy for 3D structures? Hystrix, Ital. J. Mammal. **25**(2): 73–81.

Churchill, M., Miguel, J., Beatty, B.L., Goswami, A., and Geisler, J.H. 2019. Asymmetry drives modularity of the skull in the common dolphin (Delphinus delphis). Biol. J. Linn. Soc. **126**(2): 225–239. Oxford University Press UK.

Clark, S.T., and Odell, D.K. 1999. Nursing behaviour in captive false killer whales (Pseudorca crassidens). Aquat. Mamm. **25**: 183–191. EUROPEAN ASSOCIATION FOR AQUATIC MAMMALS.

Coombs, E.J., Clavel, J., Park, T., Churchill, M., and Goswami, A. 2020. Wonky whales: the evolution of cranial asymmetry in cetaceans. BMC Biol. **18**(1): 1–24. BioMed Central.

Cozzi, B., Huggenberger, S., and Oelschläger, H.A. 2016. Anatomy of dolphins: insights into body structure and function. Academic Press.

Cranford, T. 1999. THE SPERM WHALE'S NOSE: SEXUAL SELECTION ON A GRAND SCALE? 1. Mar. mammal Sci. **15**(4): 1133–1157. Wiley Online Library.

Cranford, T.W., Amundin, M., and Krysl, P. 2015. Sound production and sound reception in delphinoids. Dolphin Commun. Cogn. Past, Present. Futur. **328**. MIT Press.

Cranford, T.W., Amundin, M., and Norris, K.S. 1996. Functional morphology and homology in the odontocete nasal complex: implications for sound generation. J. Morphol. **228**(3): 223–285. Wiley Online Library.

Cranford, T.W., and Krysl, P. 2018. Sound paths, cetaceans. *In* Encyclopedia of Marine Mammals. Elsevier. pp. 901–904.

Cranford, T.W., Mckenna, M.F., Soldevilla, M.S., Wiggins, S.M., Goldbogen, J.A., Shadwick, R.E., Krysl, P., St. Leger, J.A., and Hildebrand, J.A. 2008. Anatomic geometry of sound transmission and reception in Cuvier's beaked whale (Ziphius cavirostris). Anat. Rec. Adv. Integr. Anat. Evol. Biol. Adv. Integr. Anat. Evol. Biol. **291**(4): 353–378. Wiley Online Library.

del Castillo, D.L., Flores, D.A., and Cappozzo, H.L. 2014. Ontogenetic development and sexual dimorphism of franciscana dolphin skull: A 3D geometric morphometric approach. J. Morphol. **275**(12): 1366–1375. Wiley Online Library.

del Castillo, D.L., Segura, V., Flores, D.A., and Cappozzo, H.L. 2016. Cranial development and directional asymmetry in Commerson's dolphin, Cephalorhynchus commersonii commersonii: 3D geometric morphometric approach. J. Mammal. **97**(5): 1345–1354. Oxford University Press US.

del Castillo, D.L., Viglino, M., Flores, D.A., and Cappozzo, H.L. 2017. Skull ontogeny and modularity in two species of Lagenorhynchus: Morphological and ecological

implications. J. Morphol. **278**(2): 203–214. Wiley Online Library.

Duffield, D.A. 1988. Demographic features of killer whales in oceanaria in the United States and Canada, 1965-1987. North Atl. Kill. Whales: 297–306. Rit Fiskideildar.

Fahlke, J.M., Gingerich, P.D., Welsh, R.C., and Wood, A.R. 2011. Cranial asymmetry in Eocene archaeocete whales and the evolution of directional hearing in water. Proc. Natl. Acad. Sci. **108**(35): 14545–14548. National Acad Sciences.

Fahlke, J.M., and Hampe, O. 2015. Cranial symmetry in baleen whales (Cetacea, Mysticeti) and the occurrence of cranial asymmetry throughout cetacean evolution. Sci. Nat. **102**(9–10): 58. Springer.

Ferreira, I.M. 2008. Growth and reproduction in false killer whales (Pseudorca crassidens Owens, 1846). Faculty of Natural and Agricultural Science, University of Pretoria, South Africa. M. Sc. Thesis: 152.

Ferreira, I.M. 2009 Growth and reproduction in false killer whales (*Pseudorca crassidens* Owens, 1846). Diss. University of Pretoria.

Ferreira, I.M., Kasuya, T., Marsh, H., and Best, P.B. 2014. False killer whales (Pseudorca crassidens) from Japan and South Africa: Differences in growth and reproduction. Mar. Mammal Sci. **30**(1): 64–84. Wiley Online Library.

Figueirido, B., Tseng, Z.J., and Martín-Serra, A. 2013. Skull shape evolution in durophagous carnivorans. Evolution (N. Y). **67**(7): 1975–1993. Wiley Online Library.

de Francesco, M.C., and Loy, A. 2016. Intra-and Interspecific Interactions as Proximate Determinants of Sexual Dimorphism and Allometric Trajectories in the Bottlenose Dolphin Tursiops truncatus (Cetacea, Odontoceti, Delphinidae). PLoS One **11**(10): e0164287. Public Library of Science San Francisco, CA USA.

Fruciano, C. 2016. Measurement error in geometric morphometrics. Dev. Genes Evol. **226**(3): 139–158. Springer.Galatius, A. 2010. Paedomorphosis in two small species of toothed whales (Odontoceti): how and why? Biol. J. Linn. Soc. **99**(2): 278–295. Oxford University Press.

Galatius, A., and Goodall, R.N.P. 2016. Skull shapes of the Lissodelphininae: radiation, adaptation and asymmetry. J. Morphol. **277**(6): 776–785. Wiley Online Library.

590 Galatius, A., Racicot, R., McGowen, M., and Olsen, M. T. (2020). Evolution and
591 diversification of delphinid skull shapes. Iscience, 23(10), 101543

592 Garde, E., Heide-Jørgensen, M.P., Hansen, S.H., Nachman, G., and Forchhammer, M.C. 2007.
593 Age-specific growth and remarkable longevity in narwhals (Monodon monoceros) from
594 West Greenland as estimated by aspartic acid racemization. J. Mammal. **88**(1): 49–58.
595 American Society of Mammalogists 810 East 10th Street, PO Box 1897, Lawrence ….

596 Gol'din, P., and Vishnyakova, K. 2016. Habitat shapes skull profile of small cetaceans:
597 evidence from geographical variation in Black Sea harbour porpoises (Phocoena
598 phocoena relicta). Zoomorphology **135**(3): 387–393. Springer.

599 Goldbogen, J.A., Cade, D.E., Wisniewska, D.M., Potvin, J., Segre, P.S., Savoca, M.S., Hazen,
600 E.L., Czapanskiy, M.F., Kahane-Rapport, S.R., and DeRuiter, S.L. 2019. Why whales are
601 big but not bigger: Physiological drivers and ecological limits in the age of ocean giants.
602 Science (80-.). **366**(6471): 1367–1372. American Association for the Advancement of
603 Science.

604 Hallgrímsson, B., Willmore, K., and Hall, B.K. 2002. Canalization, developmental stability,
605 and morphological integration in primate limbs. Am. J. Phys. Anthropol. Off. Publ. Am.
606 Assoc. Phys. Anthropol. **119**(S35): 131–158. Wiley Online Library.

607 Huggenberger, S., Leidenberger, S., and Oelschläger, H.H.A. 2017. Asymmetry of the
608 nasofacial skull in toothed whales (Odontoceti). J. Zool. **302**(1): 15–23. Wiley Online
609 Library.

610 Jensen, F.H., Johnson, M., Ladegaard, M., Wisniewska, D.M., and Madsen, P.T. 2018. Narrow
611 Acoustic Field of View Drives Frequency Scaling in Toothed Whale Biosonar. Curr. Biol.
612 **28**(23): 3878–3885. Elsevier.

613 Kastelein, R.A., Mosterd, J., Schooneman, N.M., and Wiepkema, P.R. 2000. Food
614 consumption, growth, body dimensions, and respiration rates of captive false killer whales
615 (Pseudorca crassidens). Aquat. Mamm. **26**(1): 33–44. EUROPEAN ASSOCIATION FOR
616 AQUATIC MAMMALS.

617 Kitchener, D.J., Ross, G.J.B., and Caputi, N. 1990. Variation in skull and external morphology
618 in the false killer whale, *Pseudorca crassidens*, from Australia, Scotland and South Africa.
619 Mammalia **54**(1): 119–136. Walter de Gruyter, Berlin/New York.

620 Klingenberg, C.P, and Monteiro, L.R. 2005 Distances and directions in multidimensional shape
621 spaces: implications for morphometric applications. Systematic Biology 54.4: 678-688.

622 Klingenberg, C.P. 2008. Morphological integration and developmental modularity. Annu. Rev.
623 Ecol. Evol. Syst. **39**: 115–132. Annual Reviews.

624 Klingenberg, C.P. 2009. Morphometric integration and modularity in configurations of
625 landmarks: tools for evaluating a priori hypotheses. Evol. Dev. **11**(4): 405–421. Wiley
626 Online Library.

627 Klingenberg, C.P. 2011. MorphoJ: An integrated software package for geometric
628 morphometrics. Mol. Ecol. Resour. doi:10.1111/j.1755-0998.2010.02924.x.

629 Klingenberg, C.P., Barluenga, M., and Meyer, A. 2002. Shape analysis of symmetric
630 structures: quantifying variation among individuals and asymmetry. Evolution (N. Y).
631 **56**(10): 1909–1920. Wiley Online Library.

632 Klingenberg, C.P., and Marugán-Lobón, J. 2013. Evolutionary covariation in geometric
633 morphometric data: analyzing integration, modularity, and allometry in a phylogenetic
634 context. Syst. Biol. **62**(4): 591–610. Oxford University Press.

635 Klingenberg, C.P., Mebus, K., and Auffray, J. 2003. Developmental integration in a complex
636 morphological structure: how distinct are the modules in the mouse mandible? Evol. Dev.
637 **5**(5): 522–531. Wiley Online Library.

638 Kloepper, L.N., Nachtigall, P.E., Donahue, M.J., and Breese, M. 2012. Active echolocation
639 beam focusing in the false killer whale, Pseudorca crassidens. J. Exp. Biol. **215**(8): 1306–
640 1312. The Company of Biologists Ltd.

641 Lockyer, C. 2003. Harbour porpoises (Phocoena phocoena) in the North Atlantic: Biological
642 parameters. NAMMCO Sci. Publ. **5**: 71–89.

643 Lockyer, C., Heide-Jørgensen, M.P., Jensen, J., and Walton, M.J. 2003. Life history and
644 ecology of harbour porpoises (Phocoena phocoena) from West Greenland. NAMMCO
645 Sci. Publ. **5**: 177–194.

646 Loy, A., Tamburelli, A., Carlini, R., and Slice, D.E. 2011. Craniometric variation of some
647 Mediterranean and Atlantic populations of Stenella coeruleoalba (Mammalia,
648 Delphinidae): A three-dimensional geometric morphometric analysis. Mar. Mammal Sci.
649 **27**(2): E65–E78. Wiley Online Library.

650 MacLeod, C.D. 2002. Possible functions of the ultradense bone in the rostrum of Blainville's
651 beaked whale (Mesoplodon densirostris). Can. J. Zool. **80**(1): 178–184. NRC Research
652 Press.

653 MacLeod, C.D. 2010. The relationship between body mass and relative investment in testes
654 mass in cetaceans: implications for inferring interspecific variations in the extent of sperm
655 competition. Mar. mammal Sci. **26**(2): 370–380. Wiley Online Library.

656 MacLeod, C.D., and MacLeod, R.C. 2009. The relationship between body mass and relative
657 investment in testes mass in amniotes and other vertebrates. Oikos **118**(6): 903–916.
658 Wiley Online Library.

659 MacLeod, C.D., Reidenberg, J.S., Weller, M., Santos, M.B., Herman, J., Goold, J., and Pierce,
660 G.J. 2007. Breaking symmetry: the marine environment, prey size, and the evolution of
661 asymmetry in cetacean skulls. Anat. Rec. Adv. Integr. Anat. Evol. Biol. Adv. Integr. Anat.
662 Evol. Biol. **290**(6): 539–545. Wiley Online Library.

663 MacLeod, C.D., Santos, M.B., Lopez, A., and Pierce, G.J. 2006. Relative prey size
664 consumption in toothed whales: implications for prey selection and level of specialisation.
665 Mar. Ecol. Prog. Ser. **326**: 295–307.

666 Marcus, L., Hingst-Zaher, E., and Zaher, H. 2000. Application of landmark morphometrics to
667 skulls representing the orders of living mammals. Hystrix, Ital. J. Mammal. **11**(1).

668 Marino, L., McShea, D.W., and Uhen, M.D. 2004. Origin and evolution of large brains in
669 toothed whales. Anat. Rec. Part A Discov. Mol. Cell. Evol. Biol. An Off. Publ. Am. Assoc.
670 Anat. **281**(2): 1247–1255. Wiley Online Library.

671 Marroig, G., and Cheverud, J.M. 2001. A comparison of phenotypic variation and covariation
672 patterns and the role of phylogeny, ecology, and ontogeny during cranial evolution of New
673 World monkeys. Evolution (N. Y). **55**(12): 2576–2600. Wiley Online Library.

674 Marshall, C.D. 2009. Feeding morphology. *In* Encyclopedia of marine mammals. Elsevier. pp.
675 406–414.

676 Martien, K.K., Baird, R.W., Chivers, S.J., Oleson, E.M., and Taylor, B.L. 2011. Population
677 structure and mechanisms of gene flow within island-associated false killer whales
678 (Pseudorca crassidens) around the Hawaiian Archipelago. NMFS NOAA US Dep.
679 Commer. Citeseer.

680 McCurry, M.R., Fitzgerald, E.M.G., Evans, A.R., Adams, J.W., and McHenry, C.R. 2017.
681 Skull shape reflects prey size niche in toothed whales. Biol. J. Linn. Soc. **121**(4): 936–
682 946. Oxford University Press UK.

683 Mclellan, W.A., Koopman, H.N., Rommel, S.A., Read, A.J., Potter, C.W., Nicolas, J.R.,
684 Westgate, A.J., and Pabst, D.A. 2002. Ontogenetic allometry and body composition of
685 harbour porpoises (Phocoena phocoena, L.) from the western North Atlantic. J. Zool.
686 **257**(4): 457–471. Wiley Online Library.

687 Mead, J.G., and Fordyce, R.E. 2009. The therian skull: a lexicon with emphasis on the
688 odontocetes. *In* Smithsonian Contributions to Zoology.

689 Mesnick, S., and Ralls, K. 2018. Sexual dimorphism. *In* Encyclopedia of marine mammals.
690 Elsevier. pp. 848–853.

691 Minamikawa, S., Watanabe, H., and Iwasaki, T. 2013. Diving behavior of a false killer whale,
692 Pseudorca crassidens, in the Kuroshio–Oyashio transition region and the Kuroshio front
693 region of the western North Pacific. Mar. mammal Sci. **29**(1): 177–185. Wiley Online
694 Library.

695 Monteiro-Filho, E.L. de A., Monteiro, L.R., and dos Reis, S.F. 2002. Skull shape and size
696 divergence in dolphins of the genus Sotalia: a tridimensional morphometric analysis. J.
697 Mammal. **83**(1): 125–134. American Society of Mammalogists 810 East 10th Street, PO
698 Box 1897, Lawrence ….

699 Murphy, S., A. Collet, and E. Rogan. 2005 "Mating strategy in the male common dolphin
700 (Delphinus delphis): what gonadal analysis tells us." *Journal of Mammalogy* 86.6: 1247-
701 1258.

702 Murphy, S., and Rogan, E. 2006. External morphology of the short-beaked common dolphin,
703 Delphinus delphis: Growth, allometric relationships and sexual dimorphism. Acta Zool.
704 **87**(4): 315–329. Wiley Online Library.

705 Murray, S.O., Mercado, E., and Roitblat, H.L. 1998. The neural network classification of false
706 killer whale (Pseudorca crassidens) vocalizations. J. Acoust. Soc. Am. **104**(6): 3626–
707 3633. Acoustical Society of America.

708 Nicolosi, P., and Loy, A. 2010. Landmark based morphometric variation in Common dolphin
709 (Delphinus delphis L., 1758). EUT Edizioni Università di Trieste.

710 Nowak, R.M., and Walker, E.P. 1999. Walker's Mammals of the World. JHU press.

711 Odell, D.K., and McClune, K.M. 1999. False killer whale Pseudorca crassidens (Owen, 1846).
712 Handb. Mar. Mamm. **6**: 213–243. Academic Press.

713 Oswald, J.N., Barlow, J., and Norris, T.F. 2003. Acoustic identification of nine delphinid
714 species in the eastern tropical Pacific Ocean. Mar. mammal Sci. **19**(1): 20–37. Wiley
715 Online Library.

716 Ottensmeyer, C.A., and Whitehead, H. 2003. Behavioural evidence for social units in long-
717 finned pilot whales. Can. J. Zool. **81**(8): 1327–1338. NRC Research Press Ottawa,
718 Canada.

719 Palacios, D.M., and Mate, B.R. 1996. Attack by false killer whales (Pseudorca crassidens) on
720 sperm whales (Physeter macrocephalus) in the Galapagos Islands. Mar. Mammal Sci.
721 **12**(4): 582–587. Wiley Online Library.

722 Parés-Casanova, P.-M., and Fabre, L. 2013. Size and shape variability in the skull of the
723 bottlenose dolphin, Tursiops truncatus (Montagu, 1821). Anat. Histol. Embryol. **42**(5):
724 379–383. Wiley Online Library.

725 Piscitelli, M.A., McLellan, W.A., Rommel, S.A., Blum, J.E., Barco, S.G., and Pabst, D.A.
726 2010. Lung size and thoracic morphology in shallow-and deep-diving cetaceans. J.
727 Morphol. **271**(6): 654–673. Wiley Online Library.

728 Purves, P.E., and Pilleri, G. 1978. The functional anatomy and general biology of Pseudorca
729 crassidens (Owen) with a review of the hydrodynamics and acoustics in Cetacea. Investig.
730 Cetacea **9**: 67–227. Institute of Brain Anatomy, University of Berne Berne.

731 R Core Team, 2018. RStudio: R: A language and environment for statistical computing. R
732 Foundation for Statistical Computing, Vienna. https://www.R-project.org/.

733 Ralls, K. 1976. Mammals in which females are larger than males. Q. Rev. Biol. **51**(2): 245–
734 276. Stony Brook Foundation, Inc.

735 Ralls, K., and Mesnick, S. 2009. Sexual dimorphism. *In* Encyclopedia of marine mammals.
736 Elsevier. pp. 1005–1011.

737 Ramos, R.M.A., Di Beneditto, A.P.M., Siciliano, S., Santos, M.C.O., Zerbini, A.N., Bertozzi,
738 C., Vicente, A.F.C., Zampirolli, E., Alvarenga, F.S., and Lima, N.R.W. 2002. Morphology

739 of the franciscana (Pontoporia blainvillei) off southeastern Brazil: sexual dimorphism,
740 growth and geographic variation. Lat. Am. J. Aquat. Mamm. **1**(1): 129–144.

741 Read, A.J., and Gaskin, D.E. 1990. Changes in growth and reproduction of harbour porpoises,
742 Phocoena phocoena, from the Bay of Fundy. Can. J. Fish. Aquat. Sci. **47**(11): 2158–2163.
743 NRC Research Press.

744 Reeves, R.R., Smeenk, C., Brownell, R.L., and Kinze, C.C. 1999. Atlantic white-sided dolphin
745 Lagenorhynchus acutus (Gray, 1828). Handb. Mar. Mamm. Second B. Dolphins
746 Porpoises **6**: 31–56.

747 Rendell, L.E., Matthews, J.N., Gill, A., Gordon, J.C.D., and Macdonald, D.W. 1999.
748 Quantitative analysis of tonal calls from five odontocete species, examining interspecific
749 and intraspecific variation. J. Zool. **249**(4): 403–410. Wiley Online Library.

750 Riccialdelli, L., and Goodall, N. 2015. Intra-specific trophic variation in false killer whales
751 (Pseudorca crassidens) from the southwestern South Atlantic Ocean through stable
752 isotopes analysis. Mamm. Biol. **80**(4): 298–302. Elsevier.

753 Rohlf, F.J., and Marcus, L.F. 1993. A revolution morphometrics. Trends Ecol. Evol. **8**(4): 129–
754 132. Elsevier.

755 Sanino, G.P., and Fowle, H.L. 2006. Study of whistle spatio-temporal distribution and
756 repertoire of a school of false killer whales, Pseudorca crassidens, in the eastern South
757 Pacific. Boletín del Mus. Nac. Hist. Nat. **55**: 21–39.

758 Sanvicente-Añorve, L., López-Sánchez, J.L., Aguayo-Lobo, A., and Medrano-González, L.
759 2004. Morphometry and sexual dimorphism of the coastal spotted dolphin, Stenella
760 attenuata graffmani, from Bahia de Banderas, Mexico. Acta Zool. **85**(4): 223–232. Wiley
761 Online Library.

762 Seagers, D.J. 1982. Jaw structure and functional mechanics of six delphinids (Cetacea:
763 Odontoceti). [MS thesis], San Diego State Univ.

764 Shirihai, H. 2006. Whales, dolphins, and seals: A field guide to the marine mammals of the
765 world. A. & C. Black.

766 Slice, D.E. 2014. Morpheus et al. User's Guide. Available from
767 http://morphlab.sc.fsu.edu/software/morpheus/morpheus/users_guide20140704.pdf
768 [accessed 19 February 2019].

769 Sørensen, T.B., and Kinze, C.C. 1994. Reproduction and reproductive seasonality in Danish
770 harbour porpoises, Phocoena phocoena. Ophelia **39**(3): 159–176. Taylor & Francis.

771 Stacey, P.J., Baird, R.W., and Leatherwood, S. 1994. Pseudorca crassidens. Soc.

772 Stockley, P. 2004 "Sperm competition in mammals." *Human Fertility* 7.2: 91-97.

773 Tolley, K.A., Read, A.J., Wells, R.S., Urian, K.W., Scott, M.D., Irvine, A.B., and Hohn, A.A.
774 1995. Sexual dimorphism in wild bottlenose dolphins (Tursiops truncatus) from Sarasota,
775 Florida. J. Mammal. **76**(4): 1190–1198. American Society of Mammalogists 810 East
776 10th Street, PO Box 1897, Lawrence ….

777 Tomkins, J.L., and Kotiaho, J.S. 2001. Fluctuating Asymmetry. eLS. John Wiley & Sons, Ltd.

778 Veneziano, A., Meloro, C., Irish, J.D., Stringer, C., Profico, A., and De Groote, I. 2018.
779 Neuromandibular integration in humans and chimpanzees: Implications for dental and
780 mandibular reduction in Homo. Am. J. Phys. Anthropol. **167**(1): 84–96. Wiley Online
781 Library.

782 Westgate, A.J. 2007. Geographic variation in cranial morphology of short-beaked common
783 dolphins (Delphinus delphis) from the North Atlantic. J. Mammal. **88**(3): 678–688.
784 American Society of Mammalogists 810 East 10th Street, PO Box 1897, Lawrence ….

785 Wiig, Ø., Heide-Jørgensen, M.P., Laidre, K.L., Garde, E., and Reeves, R.R. 2012. Geographic
786 variation in cranial morphology of narwhals (Monodon monoceros) from Greenland and
787 the eastern Canadian Arctic. Polar Biol. **35**(1): 63–71. Springer.

788 Willmore, K.E., Roseman, C.C., Rogers, J., Cheverud, J.M., and Richtsmeier, J.T. 2009.
789 Comparison of mandibular phenotypic and genetic integration between baboon and
790 mouse. Evol. Biol. **36**(1): 19–36. Springer.

791 Wilson, B., Hammond, P.S., and Thompson, P.M. 1999. Estimating size and assessing trends
792 in a coastal bottlenose dolphin population. Ecol. Appl. **9**(1): 288–300. Wiley Online
793 Library.

794 Yamada, M. 1956. An analysis in mass osteology of the false killer whale, Pseudorca
795 crassidens (Owen) Part 1. Okajimas Folia Anat. Jpn. **28**(1–6): 451–463. Editorial Board
796 of Okajimas Folia Anatomica Japonica.

797 Zelditch, M.L., and Carmichael, C. 1989. Ontogenetic variation in patterns of developmental

and functional integration in skulls of Sigmodon fulviventer. Evolution (N. Y). **43**(4): 814–824. Wiley Online Library.

Zelditch, M.L., Swiderski, D.L., and Sheets, H.D. 2012. Geometric morphometrics for biologists: a primer. Academic Press.

Zelditch, M.L., Swiderski, D.L., and Sheets, H.D. 2013. A Practical Companion to Geometric Morphometrics for Biologists: Running analyses in freely-available software.

823 **Tables and captions**

824 **Table 1** Description of 37 landmarks taken on *Pseudorca crassidens* 3D cranium skull used in
825 the Geometric Morphometric analysis

	Landmarks homologous on the cranium
1-2	Tip of the rostrum
3-4	Anteriormost point of the premaxillary foramen
5-6	Posteriormedial point of the premaxilla
7	Anteriormost point of the medial suture between the nasal bones
8-9	Sutural triple-junction between nasal, frontal and maxilla
10	External occipital protuberance or lambdoid crest
11-12	Sutural triple-junction between supraoccipital, frontal and parietal
13-14	Posteriormost point on the temporal crest
15	*Opisthion*; middle point of the dorsal border of the *foramen magnum* on the intercondyloid notch
16-17	Dorsal tip of the occipital condyle
18-19	Lateral tip of the occipital condyle
20-21	Ventral tip of the occipital condyle
22-23	Medial tip of the paraoccipital process; ventralmost point of the paraoccipital process
24-25	Suture of pterygoid and basioccipital at the junction between pharyngeal crest and basioccipital crest
26-27	Posteroventral point of the postorbital process
28-29	Anteroventral point of the preorbital process
30-31	Anterior tip of lacrimal bone
32-33	Posteriormost point of the antorbital notch

34-35	Anteriormost point of the palatine
36-37	Posteriormost point of the upper alveolar groove

826

827

828

829

830

831

832

833

834

835

836

837

838

839

840

841

842

843

844

845

846 **Table 2** Description of 25 landmarks taken on *Pseudorca crassidens* 3D mandibles used in
847 Geometric Morphometric analysis.

	Landmarks homologous on mandible
1-2	*Pogonion*; Tip of the mandible
3	*Gnathion*, the lowest point along the midline of the mandibular symphysis
4-5	Posterior end of the alveolar groove
6-7	Anteriormost point of the mandibular foramen
8-9	Posteroventral point of the mandibular foramen
10-11	Posterodorsal point of the mandibular foramen
12-13	Dorsal tip of the coronoid process
14-15	Most anterior point of the mandibular notch
16-17	Innermost point of the condyle
18-19	Outer point of the condyle
20-21	Medialmost point of the condyle
22-23	Ventralmost extreme point of the condylar process
24-25	Posteroventral tip of the angular process

848

849

850

851

852

853

Table 3 Procrustes ANOVA on 85 specimens (crania) of *Pseudorca crassidens* to evaluate Repeatability index (*R*) as well as Fluctuating (FA) and Directional Asymmetry (DA).

Effect	**SS**	**MS**	**df**	***F***	***p***	***R***
Individual	0.26783	6.65E-05	4028	5.36	<0.0001	**0.95**
Side (DA)	0.12401	0.00243	51	195.88	<0.0001	
Ind*Side(FA)	0.04811	1.24E-05	3876	2.1	<0.0001	
Err (Rep)	0.04729	5.91E-06	8008			

Table 4 Procrustes ANOVA to test for shape differences between sexes on crania A) shape B) and residuals of allometry of 74 *Pseudorca crassidens* specimens.

	Shape ~	**df**	**SS**	**MS**	R^2	F	Z	p
A	Sex	1	0.0024	0.0024	0.0193	1.4202	1.1327	0.132
	Residuals	72	0.1223	0.0016	0.9806			
	Total	73	0.1247					
B	Sex	1	0.0026	0.0026	0.0224	1.6507	1.5929	0.057
	Residuals	72	0.1169	0.0016	0.9775			
	Total	73	0.1196					

Table 5 Procrustes ANOVA to test for slopes allometry of sexes on crania log Centroid Size (CS), Total Body Length (TBL), and shape of 74 *Pseudorca crassidens* specimens. Significance is highlighted in bold.

Shape ~	**df**	**SS**	**MS**	R^2	***F***	***Z***	***p***
CS	1	0.00517	0.00517	0.04132	3.1459	3.4733	**0.001**
Sex	1	0.00298	0.00298	0.02382	1.8135	1.8652	**0.028**
CS:Sex	1	0.00192	0.00192	0.01536	1.1692	0.6291	0.259
Residuals	70	0.11505	0.00164	0.9195			
Total	73	0.12512					
TBL	1	0.00749	0.00749	0.05988	4.6288	4.4575	**0.001**
Sex	1	0.00299	0.00299	0.02388	1.8459	1.932	**0.025**
TBL:Sex	1	0.00134	0.00134	0.01068	0.8252	-0.419	0.661
Residuals	70	0.1133	0.00162	0.90556			
Total	73	0.12512					

Table 6 Procrustes ANOVA to test for slopes allometry of sexes on mandibles log Centroid Size (CS), Total Body Length (TBL), and shape of 29 *Pseudorca crassidens* specimens.

Shape ~	**df**	**SS**	**MS**	R^2	F	Z	p
CS	1	0.00322	0.00322	0.05842	1.7004	1.4716	0.071
Sex	1	0.00175	0.00175	0.03174	0.9238	0.01438	0.474
CS:Sex	1	0.0028	0.0028	0.05091	1.4817	1.0704	0.144
Residuals	25	0.0473	0.00189	0.85893			
Total	28	0.05507					
TBL	1	0.00281	0.00281	0.0511	1.4803	1.163	0.128
Sex	1	0.00242	0.00242	0.04399	1.2743	0.75185	0.201
TBL:Sex	1	0.00231	0.00231	0.04199	1.2166	0.63567	0.262
Residuals	25	0.04752	0.0019	0.86292			
Total	28	0.05507					

Table 7 Angular comparison of Partial Least Square (PLS) vectors of block 1 (cranium) and 2 (mandible) between sexes. Significant *p*-values of these blocks of covariation trajectories between sexes are in highlighted in bold. They reflect a statistically more similar shape variation than two random vectors.

Block1	**PLS1**	**PLS2**	**PLS3**	**PLS4**
PLS1	**56.937**	81.210	85.647	84.240
	<0.00002	0.26994	0.47022	0.05357
PLS2	85.928	**57.603**	81.735	83.487
	0.60988	**0.00003**	0.29971	0.41415
PLS3	89.520	75.890	84.475	88.435
	0.95204	0.07566	0.48862	0.84457
PLS4	85.119	85.692	84.561	77.145
	0.54074	0.58927	0.49541	0.10587
Block2	**PLS1**	**PLS2**	**PLS3**	**PLS4**
PLS1	**38.785**	76.449	86.124	82.989
	<0.00001	0.17549	0.69965	0.48487
PLS2	77.996	**60.013**	88.798	81.081
	0.23058	**0.00223**	0.90479	0.37383
PLS3	67.504	79.592	88.326	89.520
	0.02330	0.29902	0.86768	0.96187
PLS4	86.546	88.328	62.253	58.737
	0.73099	0.86788	0.00483	0.00140

Figures

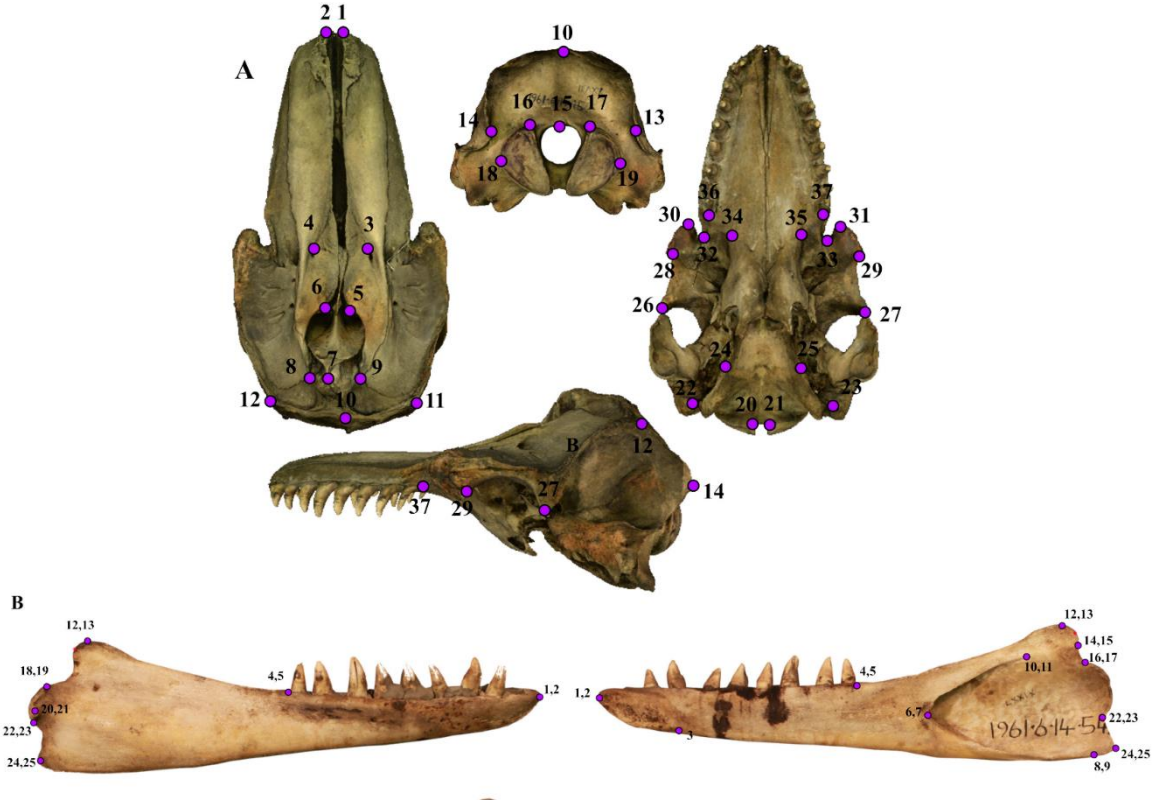

Figure 1 Landmark configuration on the A) cranium photogrammetric-based 3D model of the specimen (*Pseudorca crassidens* 1961.6.14.15 NHM, London) in dorsal, ventral, left lateral, and occipital views and B) right hemi-mandible of the specimen *Pseudorca crassidens* 1961.6.14.54 NHM, London, in labial and lingual views. See Table 1 and Table 2 for description.

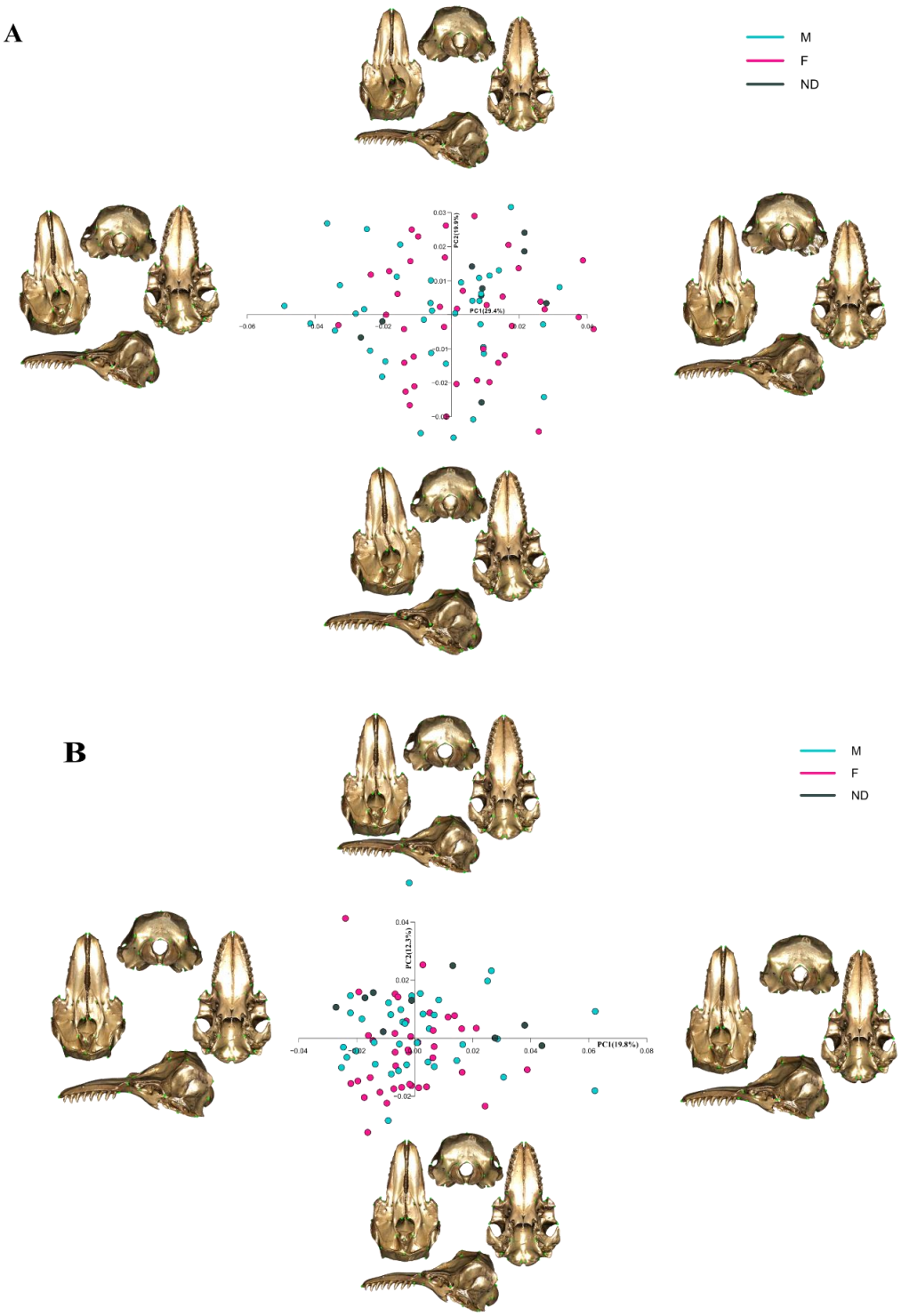

978

979 **Figure 2** Principal component plot of the asymmetric (A) and symmetric (B) component of
980 shape for 3D skull dataset. Greyscale has been used to indicates sex categories (F=females,
981 M=males, ND= no data). Shape differences along the axis of the PC1 and PC2 are visualised
982 with warping of the crania 3D models.

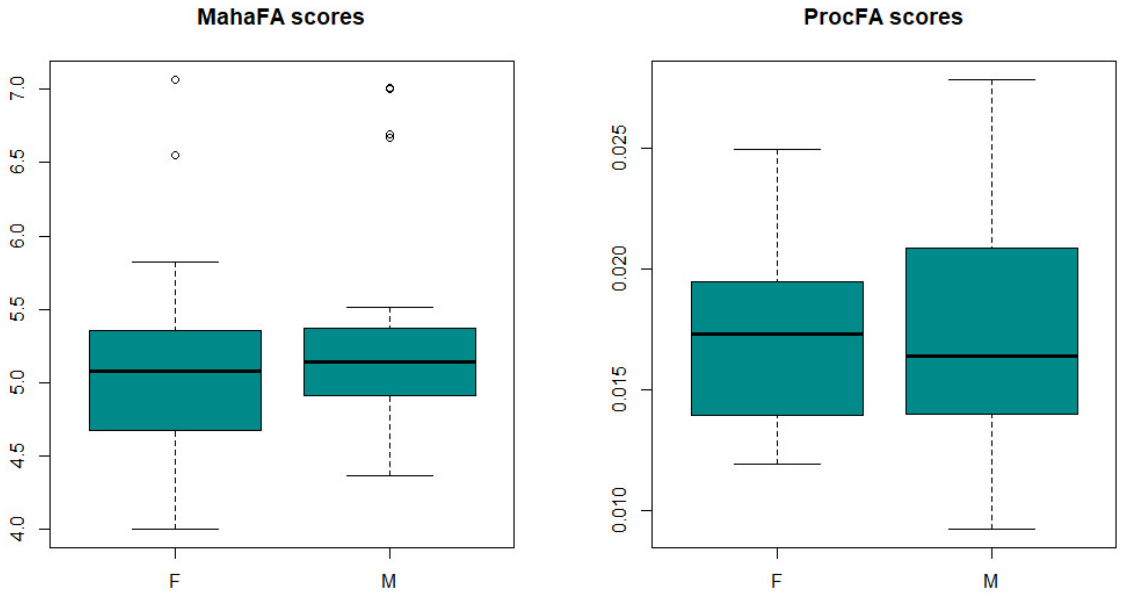

983

984

985

986 **Figure 3** Boxplots of Mahalanobis and Procrustes FA scores among female and male
987 specimens.

988

989

990

991

992

993

994

995

996

997

998

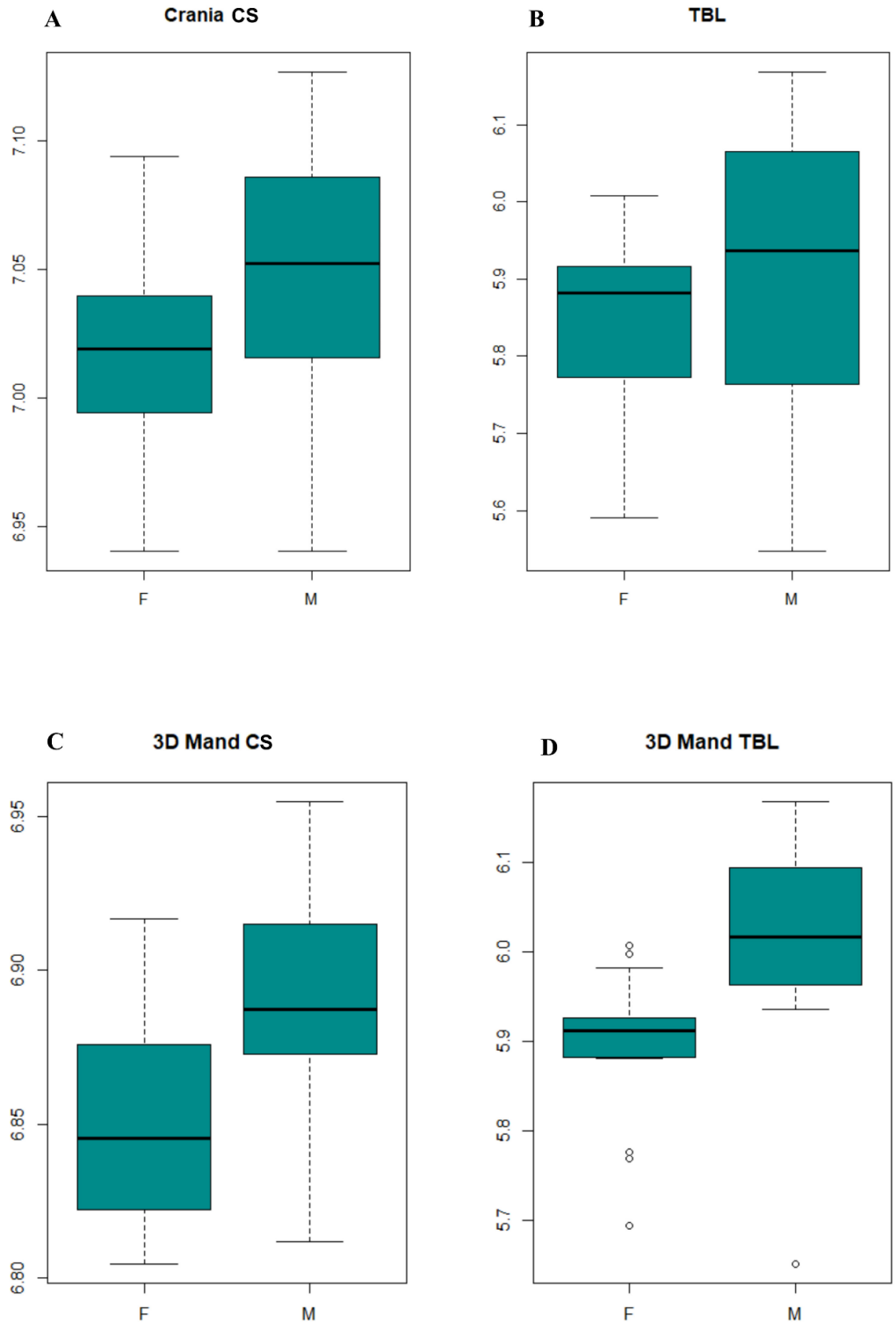

999

1000 **Figure 4** Box-whisker plots of crania dataset (*n*=74) log[CS] (A) and TBL (B) and mandibles

1001 dataset (*n*=29) log[CS] (C) and TBL (D) of females (F) and males (M) false killer whales.

1002

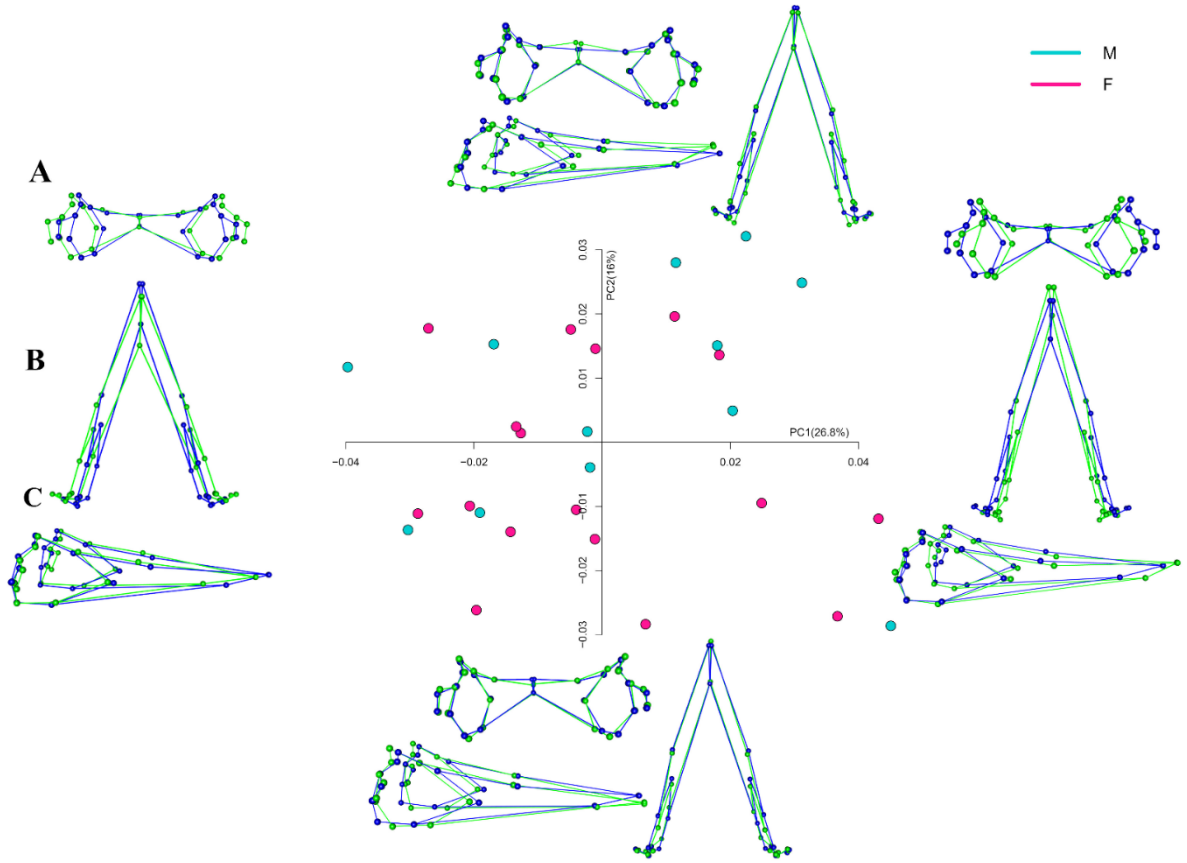

Figure 5 Principal component plot of the symmetric component of shape for 3D mandible dataset, in R. Greyscale has been used to indicates sex categories indicate sex categories (light grey F=females, dark grey M=males). Shape differences along the axis of the PC1 and PC2 can be viewed by wireframe in A) occipital, B) dental, and C) lateral view. The dark colour refers to the mean shape of the individuals while the light colour refers to the extreme individual on the negative and positive PC axes.

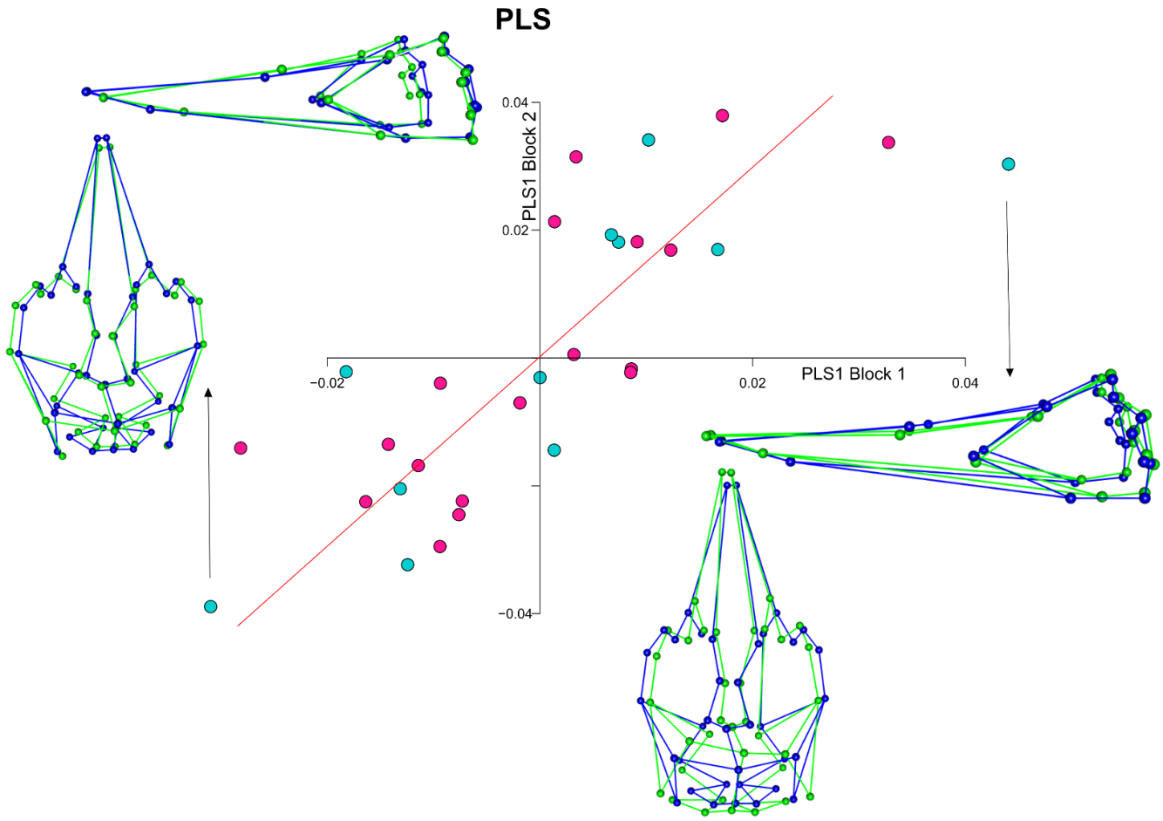

1018

1019 **Figure 6** Scatter plot of the PLS1 of block1 (Cranium) and block2 (Mandible). Shape
1020 differences can be viewed by wireframe. The dark colour refers to the mean shape of the
1021 individuals while the light colour refers to extreme most individual on the PLS1 axes.
1022 Greyscale has been used to indicates sex categories (light grey F=females, dark grey M=males).

1023